UNIVERSITÄT GRAZ

Expanding the Baum et al. (2024) model on global food production and trade: “Adaptive Shock Compensation in the Multi-layer Network of Global Food Production and Trade”

Professor: Andrew Ringsmuth
Course: Quantitative Research Methods: Complex Systems Modelling
Group: Bast Valentin, Mair Lena Valentina, Rigler Julian and Silvestri Lorenzo

Table of Contents

1. Introduction

The global food supply is made increasingly insecure by climate change. Chapter 5 of the *IPCC Special Report on Climate Change and Land* stresses that "observed climate change is already affecting food security through increasing temperatures, changing precipitation patterns, and greater frequency of some extreme events" (IPCC, 2022, 439). Rising global temperatures intensifying climate-induced weather events such as droughts, floods, and heatwaves are projected to significantly impact agricultural yields (see for example (OECD and FAO, 2022; Heilemann et al., 2024; Shi et al., 2025). This, in turn, disrupts the supply of food products with far-reaching consequences for global food security. In an era of hyperglobalization and deeply integrated global supply chains, regional agricultural failures are no longer isolated. Food production and trade systems are interconnected, meaning that yield losses or supply disruptions in one region could have direct or indirect effects on food availability in nearby regions, as well as distant parts of the world (Distefano et al., 2018). This interconnectedness heightens vulnerability to shocks and increases the risk of systemic food insecurity.

Extreme weather events from the past decades across all continents repeatedly provided evidence on the fragility of our global food system, causing significant human and economic losses. The 2010 drought in Russia decreased grain harvest by a third (Wegren, 2011) and has been linked with civil unrest in African countries due to increasing prices (Hunt et al., 2021). The prolonged drought in the Horn of Africa from 2020 to 2023, caused by five consecutive failed rainy seasons (WMO, 2023), leading to the longest drought in 40 years with crop failures and livestock losses that put over 20 million people in acute food insecurity (Odongo et al., 2025). The drought in Uruguay from 2022 to 2023, during which rainfall was over 40% below historical averages led to losses in soybean production and cattle farming, two important exports (Clevy and Evans, 2025), as well as local protests due to water shortages (Pieper, 2023). Finally, the devastating floods in Pakistan in 2022 caused by unprecedented monsoon rains submerged one third of the country, wiping out significant amounts of agricultural land and livestock (FAO, 2023), in some regions, leading to production losses of over 80% for rice (Qamer et al., 2023), a staple of which the country is one of the major exporters (Observatory of Economic Complexity, 2025). Combined, these events exemplify how climate change induced disasters have the capability of severely disrupting food production. When agricultural products are a significant export for an affected region, these losses can cascade through global supply chains, impacting the entire global food system.

Such events may, however, also happen simultaneously, as pointed out in Chapter 11.8 of the *IPCC Special Report on Climate Change and Land*: "The combination of two or more – not necessarily extreme – weather or climate events that occur: i) at the same time; ii) in close succession; or iii) concurrently in different regions, can lead to extreme impacts that are much larger than the sum of the impacts due to the occurrence of individual extremes alone. This is because multiple stressors can exceed the coping capacity of a system more quickly."

(IPCC, 2023, 1598). In such cases, one can speak of compound events, which may be different in nature, scale, and damage, but their effects are super-additive.

To address these emerging threats, it is crucial to understand how climate-induced shocks to agricultural yields propagate through the global food network and what the implications of simultaneous climate events occurring in different parts of the world are for countries across the globe. Crucially, it is not only important to understand shocks and their impact, but also how different countries respond and adapt to such shocks. Adaptations like trade re-routing, substitution between similar products, or export bans affect food availability in other countries directly and indirectly.

Baum et al. explain that food security is often assessed using price-based models (2024). These models focus on specific commodities and their trade flows. However, key commodities, such as wheat, maize or soybeans, also serve as inputs for other food production processes (Lagi et al., 2011; Bruckner et al., 2019). This highlights the need for models that capture both direct and indirect shock effects across global trade and production networks (Distefano et al., 2018; Laber et al., 2023). Traditional input-output models can help trace how products are transformed along supply chains (e.g., wheat into flour), but they are generally demand-driven and not well-suited for analyzing supply-side disruptions (Laber et al., 2023; Baum et al., 2024), such as those caused by the impacts of extreme weather events. Finally, and most importantly, Baum et al. underscore that existing models treat trade and production structures as static, overlooking countries' adaptive capacities in response to shocks.

This points to the benefits offered by a complexity science approach. With its focus on capturing nonlinear, emergent dynamics of complex systems, it may be possible to better account for feedback loops (positive and negative), interdependencies and understand adaptive behaviors by actors (Siegenfeld and Bar-Yam, 2020). Furthermore, networks, which are a common tool for analyzing complex systems in which many different components interact and the whole is greater than the sum of its parts (Estrada, 2024), are particularly suited to represent global food systems, which consist of complex trade relations between countries (Laber et al., 2023; Baum et al., 2024).

Thus, in line with a complexity science approach, our research aim is to better understand how climate change induced shocks propagate through the interconnected global food production and trade network, and how adaptive responses by states influence the dynamics of these shocks, potentially exacerbating food insecurity. Our research question is as follows: *How do cascading effects from climate-driven compound shocks affect global food availability?*

Specifically, we will focus on the above-mentioned disaster events from the past decade and a half: the 2010 Russian drought, the 2020–2023 drought in the Horn of Africa, the 2021–2023 drought in Uruguay, and the 2022 floods in Pakistan.

In order to answer our research question, we will further develop a model last updated by Baum et al. in 2024. It is a multi-layer network model of global food production and trade that captures the dynamics relevant to our research aim. This model is introduced below, followed by a section detailing our hypotheses. Next, we explain our method and our changes and adaptations to the model, with a focus on the extension of climate change-related impacts on food production and yields. After a presentation and discussion of our main results, the report ends with a conclusion.

2. The network model by Baum, et al.

The complex model by Baum, et al. (2024) simulating global food production and trade is based on a previous model developed by Laber, et al. (2023). The latter constructed a multi-layer network of food products, to understand how shocks like the Russian invasion of Ukraine could propagate through the global food system and have cascading global effects. This is particularly significant as such cascading shocks are becoming increasingly frequent (Cottrell et al., 2019; Gephart et al., 2016), with important implications for global food security. Building on the foundations provided by Laber, et al. (2023), Baum, et al. (2024) developed the model by adding the adaptive capabilities of countries to respond to shocks, thus representing a significant improvement over the earlier model. The article *Adaptive Shock Compensation in the Multi-layer Network of Global Food Production and Trade* by Sophia Baum et al. thus investigates how the global food system responds to supply shocks and how countries' responses can unintentionally exacerbate food insecurity caused by supply chains in the global trade network.

In the multi-layer network model first developed by Laber, et al (2023), each layer corresponds to a food product (such as wheat or rice). The authors incorporated 123 agricultural food products in total, thus the network consists of 123 layers. Within each layer, every node represents one country for a total of 192 in total. Edges represent trade relationships for a specific product, forming a directed and weighted network where direction indicates import or export flow, and weight reflects the volume traded. The network is therefore node-aligned, i.e. every node (country) is represented in every layer (product). It is also diagonal and categorical, as all the inter-layer edges connect a node and its counterpart in the other layer, i.e. interconnections between layers are only between one country in the product layer and its counterpart in another layer (e.g. [Austria, Wheat and products] is connected with [Austria, beer]). These inter-layer edges represent the production of secondary products, also referred to as the food transformation process.

The model is informed by robust empirical data. The authors relied on a detailed historical bilateral trade dataset, the FABIO database by Bruckner, et al. (2019) that included all 123 products across 192 countries. The products are organized in 24 product/commodity groups. One of the crucial advancements by Baum, et al. (2024) is that products within the same group can be substituted in case of a shortage. For instance, rice can be substituted with maize, as both products are part of the cereals group, or palm oil with olive oil, as both are

part of the vegetable oil group, but honey, which is the only product in its commodity group, cannot be substituted with any other product. The historical time-series data is useful as it allows to infer how countries historically adapted to past supply shocks. Furthermore, by looking at the inputs and outputs of food products into a country, the model can capture food transformation and substitution patterns, where food transformation is understood as the processing of wheat into flour, for example. In their model, Baum et al. introduce three different adaptive mechanisms: a country can either increase its imports from trading partners, scale up domestic production of the shocked products, or substitute the product with a similar product from the same group. Finally, the authors also used the Human Development Index (HDI) developed by the United Nations Development Programme to understand the impact of shocks in more versus less economically developed countries, allowing the model to predict potential distributional inequalities.

Baum et al. simulate 23616 different food shock scenarios (one per country and per food product, so 123*192). The model simulates the adaptation mechanisms across food product layers after a shock occurs. The shock propagates through the network, leading to losses in food availability in certain countries. These must adapt and adjust their imports, for example via substitution, which may lead to a higher competition for resources, which can exacerbate food inequality and lead to further losses in food availability. The model considers a diversification of the food supply as a remedy to increase a country's resilience to shocks. Figure 1 below demonstrates our own representation of the causal loop diagram of the model by Baum, et al.

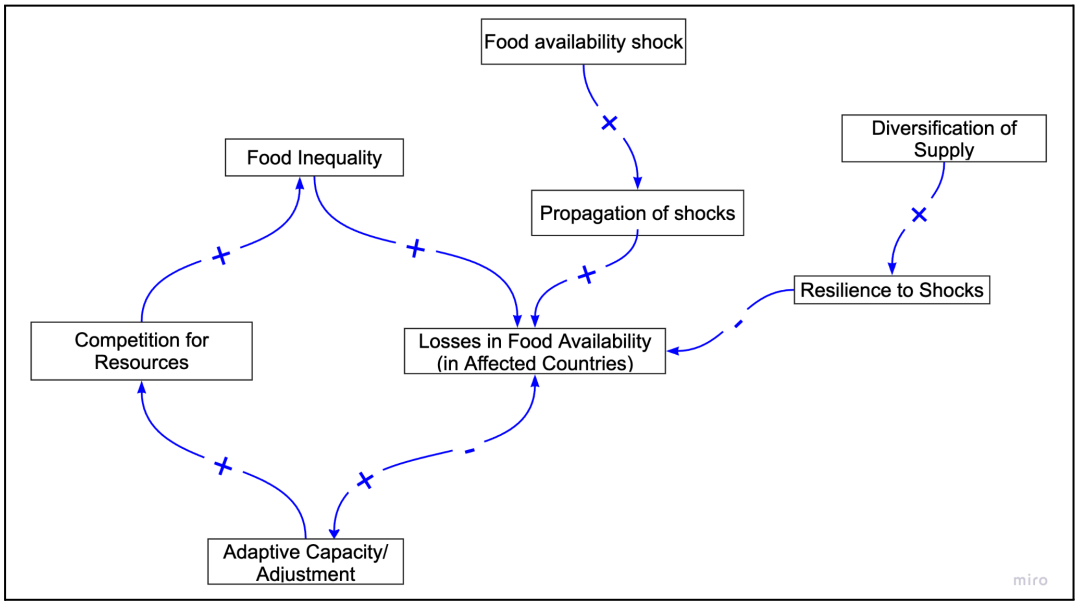

Figure 1: Causal loop diagram of the model by Baum, et al. (own representation using miro.com).

Baum et al. find that, when India introduces a ban on rice exports, countries with a lower HDI suffer the most. As a result of the Indian rice export ban, countries with a higher HDI experienced higher losses in rice imports compared to countries with a low HDI. However,

adaptation mechanisms benefit wealthier countries with more flexible, diversified food systems, often at the expense of poorer nations. Adaptive responses such as substitution or changing imports can trigger cascading shortages or redirect trade flows, which can cause spillover effects on other trade relations. These effects are often indirect and difficult to understand without a system-wide model such as the one by Baum et al. The authors find that when multiple shocks occur at the same time, their effects are super-additive, meaning that their effect is greater than when shocks are added individually. The network position of countries is crucial here, as a diversity of trade partners and food imports increases its resilience to shocks.

Model parameters

Building on the introduction above, this section details the formal parameters and computational implementation of the Baum et al. (2024) model. The model is structured around sectors (a, i). One sector represents a combination of area a (country) and item i (product). The available amount of product x_ia(t) at simulation time-step t equals the added production output and trade imports for each iteration of the simulation. With the tuple of (area, item), which is denoted as one sector, and with 192 countries and 123 different products, we get a total of 23.616 sectors.

The model parameters $\alpha^{p}_{a,i}$, $\beta^{p}_{a,i}$, $\nu_{a,i}$, $T_{a,i,b}$, $\eta^{exp}_{a,i}$, $\eta^{prod}_{a,i}$, $\eta^{cons}_{a,i}$ and the initial vector $x_{0\,a,i}$ are derived from the 2020 FABIO data. The input parameters are then fed into the models via input matrices. The output of a sector is the sum of the production processes that produce the item in that area.

The matrix alpha in the code implements the respective output rates of a production process towards sectors for processes that require production input, i.e. secondary production processes such as producing flour from wheat. The matrix beta implements the production processes that require no input, i.e. primary production processes such as growing apples. Either alpha or beta can be greater than zero for a specific process p and sector, but not both - the process is either a primary or secondary production process. The matrix nu implements the input share for process p from the for-production allocated share of sectors into the model, therefore resulting in the output of a process. Matrix matrix T indicates the shares of the for-trade reserved volumes, resulting in the amount obtained from trade which is calculated by summing the imports from trading partners from which item i is imported. At the end of a timestep each sector has the sum of output and trade available as total amount x (a,i).

The allocated shares for both production and exports are calculated by the individual shares η of each sector, the values are stored in the vector ‘eta_prod’ and then multiplied by the total amount x in sector (a,i), and eta_exp multiplied by the total amount x in sector (a,i), respectively. The model runs with tau = 10 time steps.

Before proceeding, we would like to explain the adaptation and substitution mechanisms used in the multi-layer network model by Baum et al. These are the processes that are necessary to understand our own developments and additions to the model.

Adaptation mechanism

The model assures growth adjustment for the data. Before starting the adaptation, the model first checks if an event has occurred. For this to be the case, three criteria must be fulfilled. First, there must be a substantial relative loss of the available amount, exceeding a threshold limit, defined as limit_rel_sim = 0.26. Second, there must be substantial absolute loss of the available amount, exceeding a threshold limit, defined as limit_abs_sim = 1000 tonnes. Third, the model checks for stable conditions before and after the event to avoid misinterpretation of natural variability as food shock events. Stability is quantified, the coefficient of variation (CV) must fall under the threshold of limit_dev_sim = 0.32. If these criteria are met, a food shock is classified as an event.

If the requirements of a substantial loss are fulfilled and an event has been identified, a variety of strategies for compensation dynamics can be initiated by the country as described in Bauer et al. 2024. These strategies include:

- Increasing the volume of imports by strengthening existing or establishing new trade relationships for the product.
- Adjusting the allocation of production inputs by directing more of the vulnerable product to their own production (grain for bread vs. grain as input for more grain production).
- Increasing production of vulnerable products by shifting production rates towards it.
- Shifting allocation from trade to domestic uses (reducing export).
- Increasing imports of substitutes.

After a shock has occurred and an event has been identified, changes in the parameters are observed to derive the general adaptation. A country may either adjust existing relationships (weights) (e.g. increase imports from an existing trade partner), or create new relationships (rewiring) (e.g. start importing from a new country). The model captures this with two adaptation components for any parameter v, which are denoted as w, weight adjustment, and r, rewiring component. These are calculated based on the change in the parameter before and after the event, scaled by the magnitude of the loss lE.

This adaptive rule framework allows the model to simulate realistic behavioral responses to food shocks, based on historical data. It distinguishes between strengthening existing relationships (e.g., buying more from a trusted partner) and creating new links (e.g., sourcing from a country not previously used).

The adaptation rules are calibrated as illustrated in the following process. For an exemplary parameter :

$$\nu(T_E + 1) = l_E \, \omega \, \nu(T_E) + l_E \, r$$

where $\nu(T_E + 1)$ relates to the parameter after the loss and $\nu(T_E)$ to the original parameter before the loss, l_E is the experienced loss at the event, ω is the adjustment in trade-relationships, and r describes the rewiring of trade-relationships.

The adaptive changes fall into two categories: reweighing and rewiring.

Reweighting means that a country intensifies its use of an already existing relationship in response to a shock. In the model, there is a change in the weight of an edge in the trade network, where the edge already exists, and now the country increases the value (flow amount), but the structure of the network has not changed. This can be described as a quantitative adjustment of an existing link. This is done by strengthening trade ties, increasing allocation of shares (in the eta matrices) or enhancing production efficiency (alpha and beta). If a connection existed before (v(T_E) > 0), reweighting scales it:

$$\omega = \frac{1}{l_E} \frac{\upsilon(T_E+1)}{\upsilon(T_E)} \qquad \text{if } \upsilon(T_E) > 0, \text{ otherwise } 0$$

Rewiring refers to establishing entirely new links. This can be done either by starting to trade with a new country, using a new production input or substituting a product that has not been used before. In the model, a new edge is added to the network, a connection that did not exist before the event. Therefore, a new source is created to compensate for the shock. This is a qualitative adjustment that changes the network structure. This is done by forming new trade links, introducing new production inputs and switching to new substitute products. The rewiring component captures how much of the post-shock response came from entirely new channels. If the parameter was zero before the shock and is nonzero after:

$$r = \frac{1}{l_E} \upsilon(T_E) \qquad \text{if } \upsilon(T_E + 1) = 0, \text{ otherwise } 0$$

Reweighting and rewiring are both scaled by the loss magnitude in the affected sector. Reweighting involves an adjustment to the strength of existing parameter values and includes a comparison of the parameters before and after the event. Rewiring, by contrast, represents the formation of new connections and is determined by multiplying the loss magnitude with the post-event parameter value, assuming the parameter was zero before the event. The parameters in the model α, β, ν, T, η_exp, and η_prod are all subject to reweighting and rewiring in this way. General reweighting and rewiring rules can be derived by averaging the corresponding w and r values across a collection of event sectors for each parameter, except for the trade matrix T. Since T does not contain item-specific information (it is country-to-country, not product-specific), averaging across items would eliminate important

structural details. Therefore, for trade parameters, the averaging is performed at the country level, based on events observed within each country. Annex 1 shows the Python code implementing the adaptation mechanism.

Substitution mechanism

First, products within the same commodity groups, according to Bruckner et al., 2019, are assumed to be similar and thus treated as potential substitutes, as shown in Figure 2. The table used to generate the figure, with the full product names, is found in Annex 2.

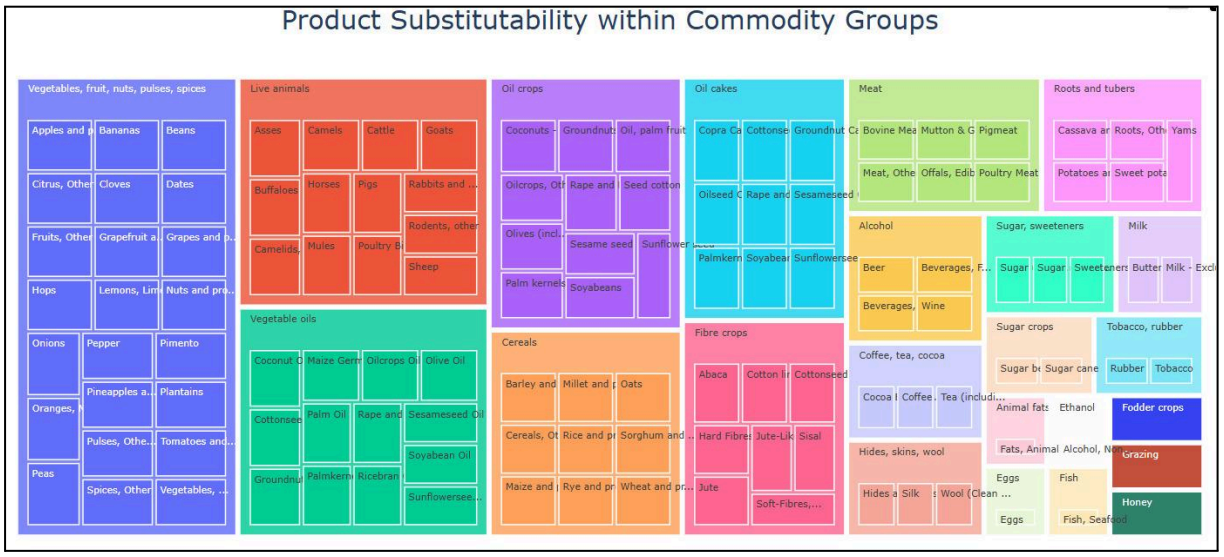

Figure 2: Products and Commodity Groups. Products within the same commodity group can be substituted (own representation). The same data is presented more clearly in Annex 2.

To calculate which products to substitute with others, first a trade import index I^{j}_{aE} is defined that consists of all items j similar to the event item in event country a_E by summing over the relevant import indices. To be included in the sum the country must be a substantial importer from the other country of at least 0.1% of the sector's exports. The mean relative change of the I^{j}_{aE} is calculated by averaging over all events affecting sectors of item i_E giving the substitutability index $s_{i E j}$. So basically we let the model run for an event, changes for the substitutes are derived, averaged over and the result will be a substitutability index. Done for all sectors and areas this will give us the substitutability index matrix $S^{a}_{i E j}$.

Substitutability index adjustment is applied when a sector has lost a substantial proportion and quantity and has not been able to recover through adjustment at timestep t = 1 and is applied at timestep t = 2. It will again apply if the relative and absolute change as well as the coefficient meet their threshold after t = 1. It is applied to the trade matrix T in the following way:

$$T^{j}_{a S b, adap} = (1 + S^{a}_{i S j}) \, T^{j}_{a S b, orig}$$

where $T^{j}_{a\,S\,b,\,orig}$ relates to the trade matrix after the adaptation mechanism. Annex 3 shows the code demonstrating the substitution mechanism.

Using this extensive multiplex model of global food production and trade, we aim to explore how compound climate-related shocks propagate through the interconnected food system, and how constraints on production capacity shape countries' adaptive responses. We aim to simulate climate-disaster induced food shocks in the global food network and understand which countries and products will experience the highest losses.

3. Hypotheses

In order to answer the research question, we developed two hypotheses. We are ultimately testing the hypotheses that climate hazards produce super-additive impacts on food availability (H1) and that realistic production limits reduce the system's resilience to cascading shocks (H2). This section details our two hypotheses.

H1: Climate Hazards Decrease Food Availability through Compound, Super-Additive Effects
Climate change is dramatically increasing the frequency, severity, and simultaneity of extreme weather events. This is posing a growing threat to global food security: floods wash away crops and the soil, droughts diminish harvests profoundly due to limited water availability and heat stress on the crops. While the global food system has become more interconnected and efficient through trade and technological advancement, this same connectivity increases systemic vulnerability (Nyström et al., 2019). Evidence suggests that food shocks caused by climate hazards, such as droughts, floods, and heatwaves, do not only occur in isolation but increasingly interact in time and space, increasing the probability of compound climate events to occur that produce super-additive effects on food production and availability (Gaupp et al., 2020).

Compound climate events refer to situations where multiple climate-related factors or hazards interact, either simultaneously or sequentially, to produce more severe impacts than each would individually. An increased probability of climate extreme events occurring both with increased frequency and with higher severity also increases the likelihood of those events happening compounded. According to the IPCC (cited in Simpson et al., 2023), these can be categorized into four main types: 1) Preconditioned events, where an initial state makes a system more vulnerable to a subsequent hazard, e.g. rain on snow events make flooding more severe due to the additional melting of the snow. 2) Multivariate events, where multiple climate hazards occur at the same time, intensifying the impact, e.g. coastal storm surge combined with heavy inland rainfall leading to extreme flooding. 3) Temporally compounding events, where multiple events occur in sequence with cumulative effects, e.g. repeated crop-damaging droughts in successive seasons leading to food insecurity. 4) Spatially compounding events, where events occur in multiple distant regions simultaneously, stressing globally distributed systems. Traditional risk models often consider one hazard at a time, but especially for food security, it is important to look into compound events, which are

more frequent and severe under climate change. These combinations can overwhelm adaptation capacities (Simpson et al., 2023).

Our hypothesis focuses particularly on spatially compounding events, where simultaneous food production shocks in different regions interact and ripple through the global food trade network. Empirical studies support this concern: the potential for climatic extremes to strike multiple breadbasket regions simultaneously has been widely recognized. Gaupp et al. (2020) show that the probability of simultaneous failure in major crops like wheat, maize, and soybean is increasing, which could drastically reduce global food availability and amplify food insecurity. While climate change poses a growing threat to global food systems, the extent to which adaptation measures can mitigate these risks remains uncertain (Hultgren et al., 2025). The impacts of extreme weather events on the global food system are further magnified by the growing concentration of food production in key exporting regions, a very globalized food trade network, which is highly connected and leads to food shocks propagating by trade to other regions of the world (Nyström et al., 2019). When climate hazards strike these regions simultaneously, they can collectively undermine the supply of globally traded staples, pushing up food prices and triggering shortages far beyond the directly affected countries.

This leads to the phenomenon of super-additivity, a mathematical concept where the total impact of combined events is greater than the sum of individual effects. In the context of food systems, this means that if two breadbasket regions experience climate-related crop losses simultaneously, the resulting global food loss is not simply the sum of the two, but is multiplied through disrupted trade, reduced substitution options and loss propagation. When wheat fails in Russia and rice fails in Pakistan at the same time, their adaptive options are limited, the adaptive capacity of substitutes of the same product group becomes scarce. These are systemic bottlenecks and are mounting pressure on humanitarian systems.

While trade and product substitution such as also simulated in the model can buffer isolated shocks, the capacity of these mechanisms is limited in the face of compound events. Highly connected food trade networks mean that shocks can propagate faster and further than in less globalized systems. Once thresholds are crossed, i.e. when too many sectors (crops or regions) are affected at the same time, adaptive responses become insufficient, resulting in sustained losses in food availability, nutritional insecurity and even famine and humanitarian crises.

We hypothesize that when realistic compound climate hazards are introduced into the global food network model, they will lead to nonlinear, super-additive declines in food availability. The simultaneous loss of adaptive capacity across multiple regions will overwhelm substitution and trade pathways, triggering systemic cascading effects of loss that significantly reduce resilience and increase the global burden of food insecurity.

H2: Implementing realistic production caps reduces the global food system's resilience to cascading shocks.

Our second hypothesis relates to planetary boundaries. Historically, global food production has increased significantly due to technological innovations, intensification and expansion of arable land. However, this growth trajectory is approaching critical ecological and economic limits (Springmann et al., 2018). While production volumes have still risen, the underlying productivity of ecosystems has shown signs of slowing. Constraints such as limited arable land, water scarcity, declining soil fertility, nutrient availability, biodiversity and pollinator loss and climate change impose hard boundaries on further intensification. Additionally, temporal constraints like the time required to regenerate lost biomass after disasters (e.g. regenerating tree crops following forest fires) make the idea of instant production scaling unrealistic.

In the model by Baum et al. (2024) countries facing food shocks are allowed to compensate and adapt by scaling up domestic production as one adaptation method. This mechanism assumes an unconstrained system, where food output can increase indefinitely in response to shortages. This assumption overlooks real-world limitations of ecosystems and agro-economic systems. For example, replanting perennial crops like fruit trees takes years before they yield harvestable output, and increasing production on degraded soils or in water-scarce regions may not be feasible. Moreover, gains in agricultural efficiency, such as those achieved by the Green Revolution, are showing signs of diminishing returns. In fact, during the past decade, the annual growth in agricultural output has slowed, especially when compared to the second half of the 20th century (USDA, 2023).

Nyström et al. suggest that short-term intensification of production may undermine long-term productivity and ecosystem resilience. Pushing neutral systems beyond their regenerative capacity undermines ecological stability and thereby increasing vulnerability to future food shocks. By introducing realistic production capacity limits in the model reflects this biophysical reality, and thereby grounding the simulation in more plausible ecological conditions. When the production scalability is constrained, the ability of countries to adapt by simply increasing production is constrained. As a result, countries become more reliant on other adaptation mechanisms, such as trade or product substitution, which may stress other sectors or trading partners. This constraint increases systemic interdependence and amplifies cascading effects. As a result, the inclusion of production capacity limits is expected to reveal a systemic decrease in global resilience. The system becomes more interdependent and could amplify the potential of cascading failures as shocks cannot be contained locally. Therefore, we hypothesize that introducing realistic food production constraints (production caps) into the model will reduce its overall adaptive capacity and lead to greater and more widespread losses in response to food production shocks.

4. Method: Extending the food network model by Baum et al.

To test our two hypotheses H1 and H2, we employ a quantitative research design. Based on the model developed by Baum, et al. (2024) and empirical data from the FABIO database (Bruckner et al., 2019), as well as yearly agricultural production data from FAOSTAT by the Food and Agriculture Organization of the United Nations (FAO, 2025), we developed our model to test the effects of four climate disaster events from the past decade, the 2010 Russian drought, the 2020–2023 drought in the Horn of Africa, the 2021–2023 drought in Uruguay, and the 2022 floods in Pakistan, on the global food network. We extend the model in two key ways: first, by introducing four distinct climate scenarios, where items in affected countries experience shocks based on agricultural production data, which also permits us to simulate the compound events, and second, by implementing a global production cap that serves as a planetary boundary, limiting the model's adaptation and substitution mechanisms to prevent indefinite compensation. Finally, we treat the data to visualize our outcomes. This section is structured along this sequence of steps.[1]

Introducing four climate shock scenarios

To test H1, we first introduced scenarios for four climate change induced disaster events: the 2010 Russian drought, the 2020–2023 drought in the Horn of Africa, the 2021–2023 drought in Uruguay, and the 2022 floods in Pakistan. For each event, we identified food items that experienced the highest relative production losses compared to the year prior to the disaster. Using data from the FAOSTAT database, we compared agricultural production levels in the year preceding each disaster to those during the disaster year. For multi-year droughts, we selected the year per item with the highest relative loss compared to the year prior to the drought event. This comparison allowed us to calculate the magnitude of the proportional agricultural losses (Φ) due to the climate event, using the following formula:

$$\Phi(c,i) = ({P^{pre}}_{c,i} - {P^{event}}_{c,i})/({P^{pre}}_{c,i}),$$

where P is the yearly agricultural output of a country c for a specific product item i.

For example, Pakistan had an agricultural output of "Rice and products" of 13,984,009 tonnes in 2021, which decreased to 10,983,081t in 2022 (FAO, 2025). Thus, Φ (Pakistan, Rice and products) ≈ 0.2146, meaning that Pakistan's national agricultural output of rice and rice-derived products decreased by approximately 21% between 2021 and 2022, the year of the flood. Note that Φ values are calculated at the national level, and therefore do not capture subnational variation in disaster impacts. Regional disparities, which can be significant (see Qamer et al., 2023 for the 2022 floods in Pakistan), are thus not reflected in the shock magnitude. Annex 4 lists all affected items for each country and their respective Φ values.

[1] The Python code for our model can be found at https://github.com/j-rigler/csm_project_/tree/Valentin.

For the four individual scenarios, these item-specific Φ values are treated independently and applied to the corresponding sectors in the model. Each shock is then propagated over time using an exponential decay function, meaning that the intensity of the shock gradually diminishes but continues to affect production:

$$\phi = i_0 \times e^{(-0.5 \times t)}$$

In our implementation, the impact of each shock halves with every time step, reflecting the long-term but diminishing consequences of extreme events on agricultural output. This function is based on the assumption that agricultural systems require time to recover from major disruptions such as droughts or floods (see for example FAO, 2021, 9 and 26; Van Loon et al., 2024; Das et al., 2025). We assume agricultural recovery to be nonlinear and initial losses to be more severe, while the recovery is gradual. While recognizing that the assumption of a 50% reduction per time step may be pessimistic, it provides an estimate which has also been used by (Hallegatte, 2015, see Appendix C).

In addition, we created a compound scenario that combines all four events to assess potential super-additive effects on global food system disruptions. In this scenario, all item-specific shocks from individual disaster events are aggregated into a single combined shock vector, allowing to simulate a hypothetical situation in which multiple climate-induced disasters occur within a short time frame, impacting the global food network simultaneously. The aim is to test H1, in other words, whether the combined effects of multiple events exceed the sum of their individual impacts. We thus simulated the national/regional events separately, and then the combined scenario. A baseline scenario without any shocks is always computed in the beginning of every simulation. The outcomes are relative to this baseline scenario.

Introducing a global food production cap

After creating the five different scenarios, one for each disaster event and a combined scenario, we introduce a realistic global food production cap to test our H2. While acknowledging that introducing a total production cap for each individual country and for every item per country would be a more granular implementation, we opted to introduce the global food production cap as a macro-level variable.

Historically, global food production increased rapidly due to agricultural expansion and technological innovation, such as mechanization and the Green Revolution to name some examples. However, in recent years, this growth has slowed (USDA, 2023). We derived the global production cap from the FAOSTAT database, which reported approximately 15.66 billion tonnes of processed and primary food products produced worldwide in 2023. We rounded the value, so the model starts with a global production cap allowing for a total production of processed and primary food of 16 billion tonnes. To reflect projected growth, this cap is modeled dynamically using an exponential function, increasing by 1.1% per time step, consistent with OECD/FAO projections as presented in their *Agricultural Outlook 2022-2031* where the authors estimate aggregate global agricultural production to increase by 1.1% per year (OECD and FAO, 2022, 18).

Each time step in our model represents one year.. To maintain realism and avoid overestimating long-term production capacity, we limit the model to 10 time steps. This time horizon allows for moderate production growth through mechanisms like sustainable intensification (Pretty et al., 2018) land-use expansion, or increased efficiency, without assuming any disproportionally disruptive technological breakthroughs like the Haber-Bosch process in the near future. To understand the effects of such a macro-variable capping global agricultural production, we simulate our scenarios with and without this cap.

Model outputs

To assess H1 and H2, we analyze model outputs across our five scenarios, with the global production cap variable on and off, focusing on per capita changes in food availability by country and item after the ten time steps of the simulation. We process our outputs to focus on the highest losses and highest profits per capita for the different food products. We define highest losses as any country-product combination where per capita food availability drops by more than 10 kg, a threshold indicating very severe disruptions relative to the levels prior to the shocks. These losses occur both in directly affected and indirectly affected countries, due to the rewiring mechanisms of the network. Conversely, we also want to devote particular attention to the country-product combinations where per capita availability increases after the shock. These countries benefit from the network rewiring mechanisms. We define highest profits as any country-product combination where per capita food availability increases by more than 10 kg compared to the baseline scenario.

Finally, we present two types of visual outputs: heatmaps and maps. Heatmaps show where and for what products highest losses and profits occur across the different scenarios, whereas maps are focused on one food product per scenario, visualizing the global spread of impacts. Together, these outputs allow us to illustrate how climate shocks disrupt food systems, as stipulated by our hypotheses.

Final model

We extended the multi-layer network model by Baum et al. (2024) to assess the impacts of compound climate shocks and production limits on the global food system. Four climate events (the 2010 Russian drought, 2020–2023 Horn of Africa drought, 2021–2023 Uruguay drought, and 2022 Pakistan floods) were modeled by applying proportional production losses (Φ) to the most affected items in affected countries based on FAOSTAT data. Shock intensity decays exponentially over 10 time steps to simulate a slow recovery. A combined scenario with all four shocks tested compound effects. We introduced a dynamic global production cap, starting at 16 billion tonnes and growing 1.1% per year, constraining global agricultural production to reflect planetary boundaries, limiting the system's adaptive capacity. Simulations ran over 10 time steps with and without the production cap. We analyzed per capita food availability changes, focusing on extreme losses and profits by country and product. Our main results are visualized through heatmaps and spatial maps highlighting vulnerability and adaptation patterns in the following section. Figure 3 below visualizes the algorithm used in our model.

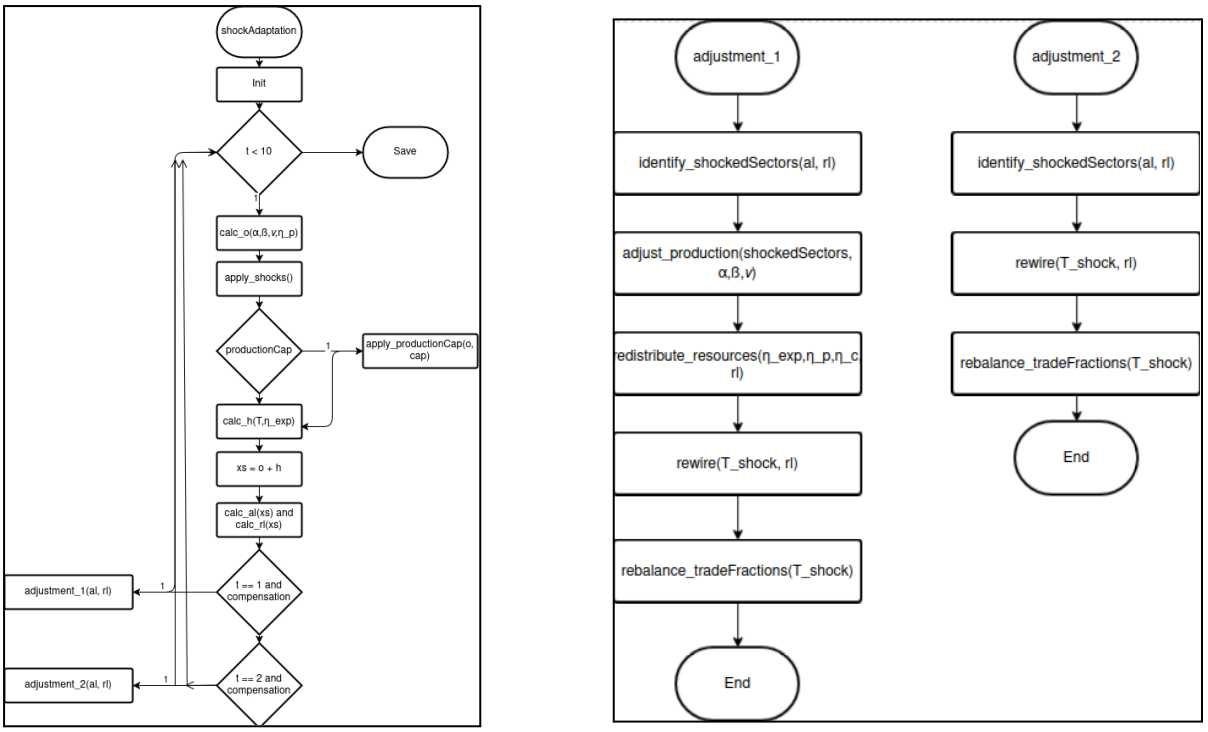

Figure 3: Visualization of our algorithm. Note: 'xs' reads 'x in shocked scenario'(on the left). Visualization of our adjustment mechanisms within the algorithm (on the right).

5. Results and discussion

This section shows our main results. We first show our results regarding the super-additivity of losses for compound climate shock events, as stipulated in our first hypothesis, then regarding our global food production cap, in line with our second hypothesis. We conclude this section by displaying curious results regarding the profits, so the products per country whose amount increased after the climate shock events.

Super-additivity of food losses

The following figure displays the losses in global production after the climate shock events. It compares the sum of the global food losses following the individual scenarios, with the global food losses following the compound shock event, where the individual shocks happen simultaneously. If super-additivity is to be observed, then the compound shock event should display a higher bar, indicating higher global food losses:

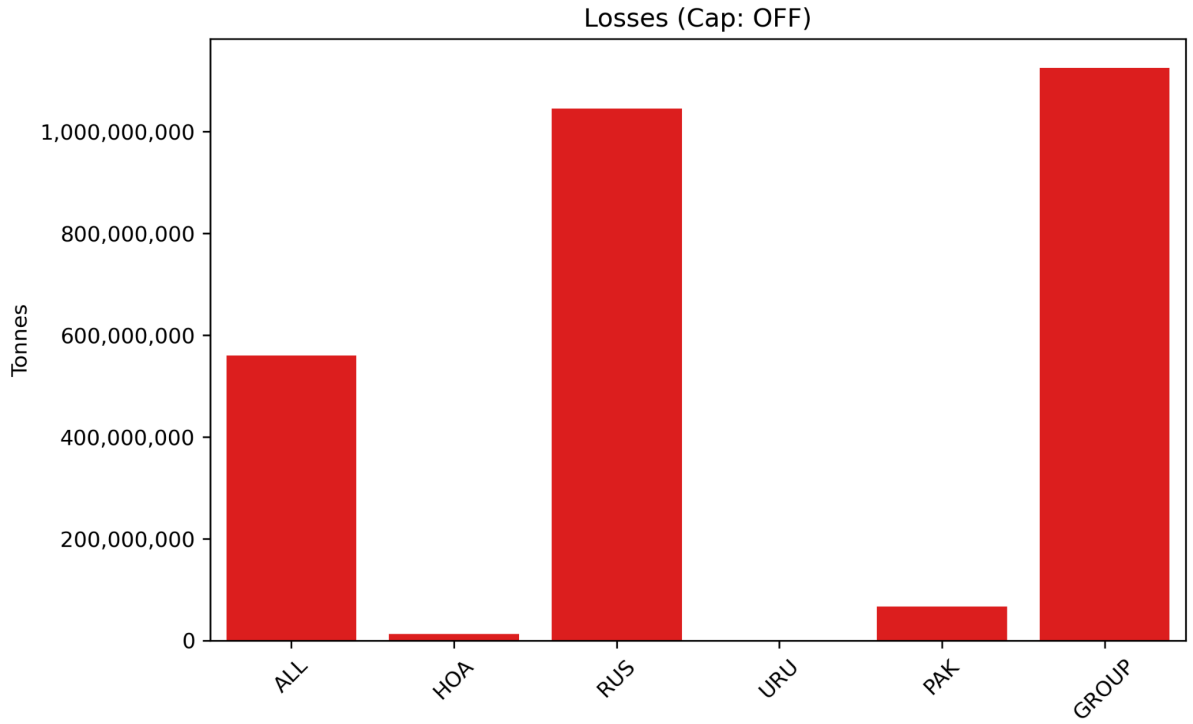

Figure 4: Comparison of total global food losses from the four individual versus the compound climate shock event (without a production cap) in tons. "Group" labels the sum of all individual scenarios. Note that a positive value indicates a loss. The higher the bar, the higher the loss in food. No super-additivity in losses is observed.

Counterintuitively the system is able to absorb losses from the compound shock better compared to when the single losses from the individual scenarios are added up to the bar we see as "GROUP" here. The magnitude of losses is also bigger for the "RUS" scenario compared to the compound scenario "ALL". This indicates that the magnitude of a shock is not as significant as the adaptation and trade-rewiring mechanism inherent to the model which may lead to the unexpected results here. So the main hypothesis of superadditive losses can not be maintained in our model. While our model applies a scaled reduction in production, Baum et al. (2024) model shocks as complete (100%) losses of specific products in affected countries, leading to a more abrupt and intense impact. Baum et al. observed superadditive losses. It could be that our climate shocks are not sufficiently strong to cause such significant losses.

Our first hypothesis (H1) expected compound climate events to produce super-additive losses in food availability across the global trade network after climate shock events. However, the results presented above indicate that the compound shock scenario resulted in food losses smaller than the sum of the individual shock scenarios. This unexpected outcome suggests that the model's adaptation mechanisms, like the reweighting and rewiring of trade and production, effectively mitigate overlapping disruptions. In other words, the network's structure enables dynamic compensation that prevents cascading failures from escalating to values that are higher than the sum of isolated shocks. The high substitutability of some

products may likely contribute to this robustness. A few limitations of this result are explained further ahead.

Introducing the global food production cap

To account for more realism with regards to global agricultural and food production, a global production capacity was introduced. When the cap is introduced, the adaptation mechanism is dimmed in a way that makes the model more realistic. But it must still be noted that the introduction of the cap on a global level and therefore the uniform rescaling of all production sectors still lacks the necessary realism to match real life. The next figure shows the total global food losses from the four individual versus the compound climate shock event once the global production cap is introduced:

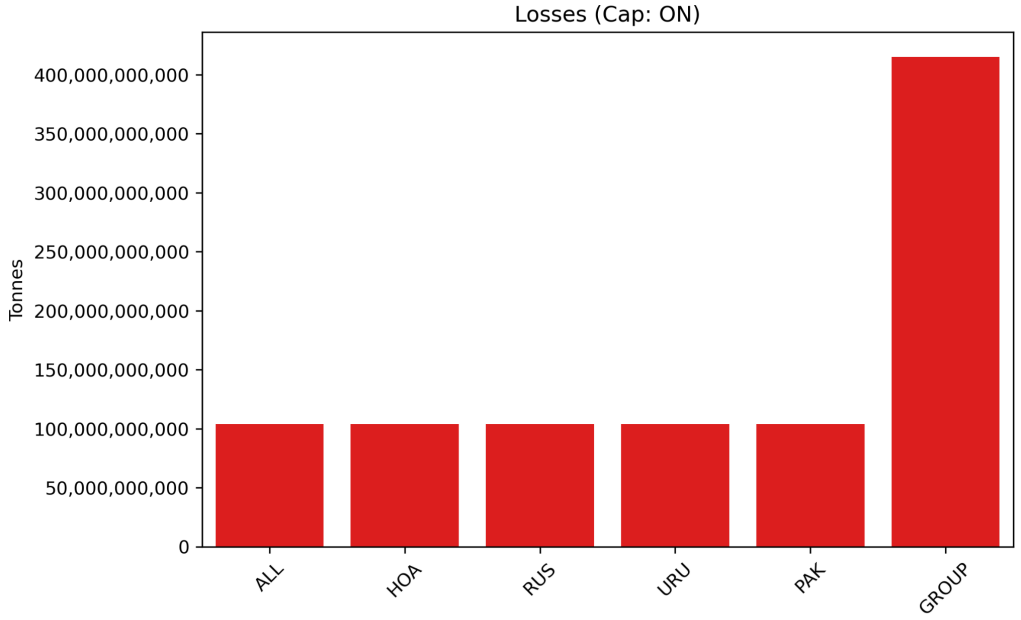

Figure 5: Comparison of global food losses from the four individual versus the compound climate shocks with a global production cap. "Group" labels the sum of all individual scenarios. Note that a positive value indicates a loss.

The figure shows the losses with a global production cap. First we can see that losses are way higher because countries can no longer just scale up production endlessly when they encounter losses in a specific sector. Again, we do not observe superadditivity of the losses which highlights the efficiency of the adaptation mechanism if it has the information of the compound damages. It is not proven here, but one can assume that the adaptation mechanism will strive to reach a certain level of acceptable losses no matter the magnitude of the damages to production in our extended model. Hence the similar loss-levels for "ALL" and the individual scenarios. Again this is different to the original model as it decreases production output to 0 when a shock occurs leading to superadditive losses.

To shed light on the significance of the production capacity the following figures are presented. We highlight two illustrative cases: first, a comparison of absolute losses per product across all affected countries following a climate shock such as the Horn of Africa

drought, second, a global map displaying absolute per capita losses of wheat and its derived products. In both cases, the outcomes are shown with and without the production cap to underscore its impact on the global food system.

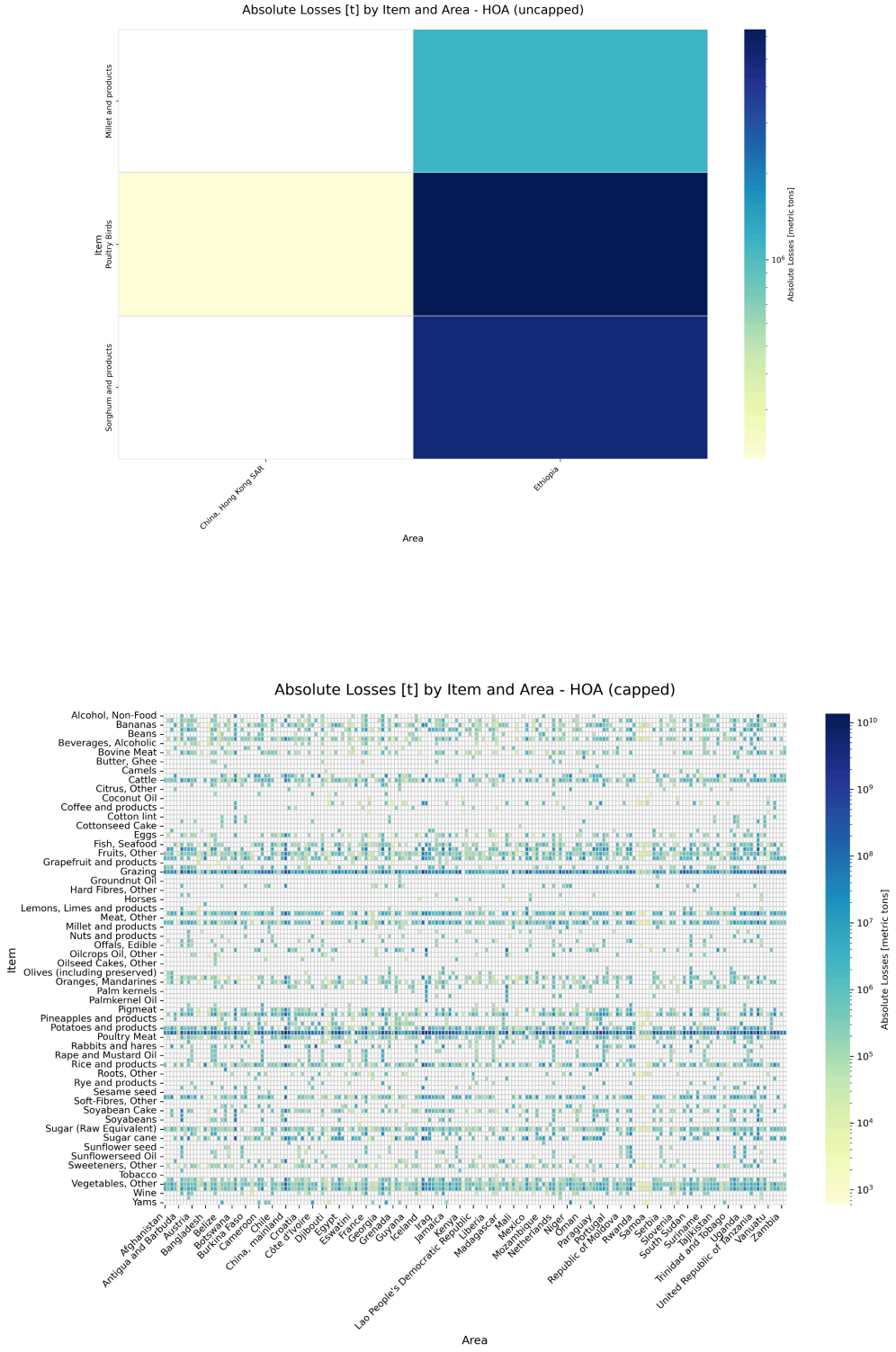

Figure 6: Absolute losses (t) in affected products by country following the Horn of Africa climate shock scenario, without a global production cap (top) and with a global production cap (bottom). Losses are calculated as the difference from amounts in the year before the disaster.

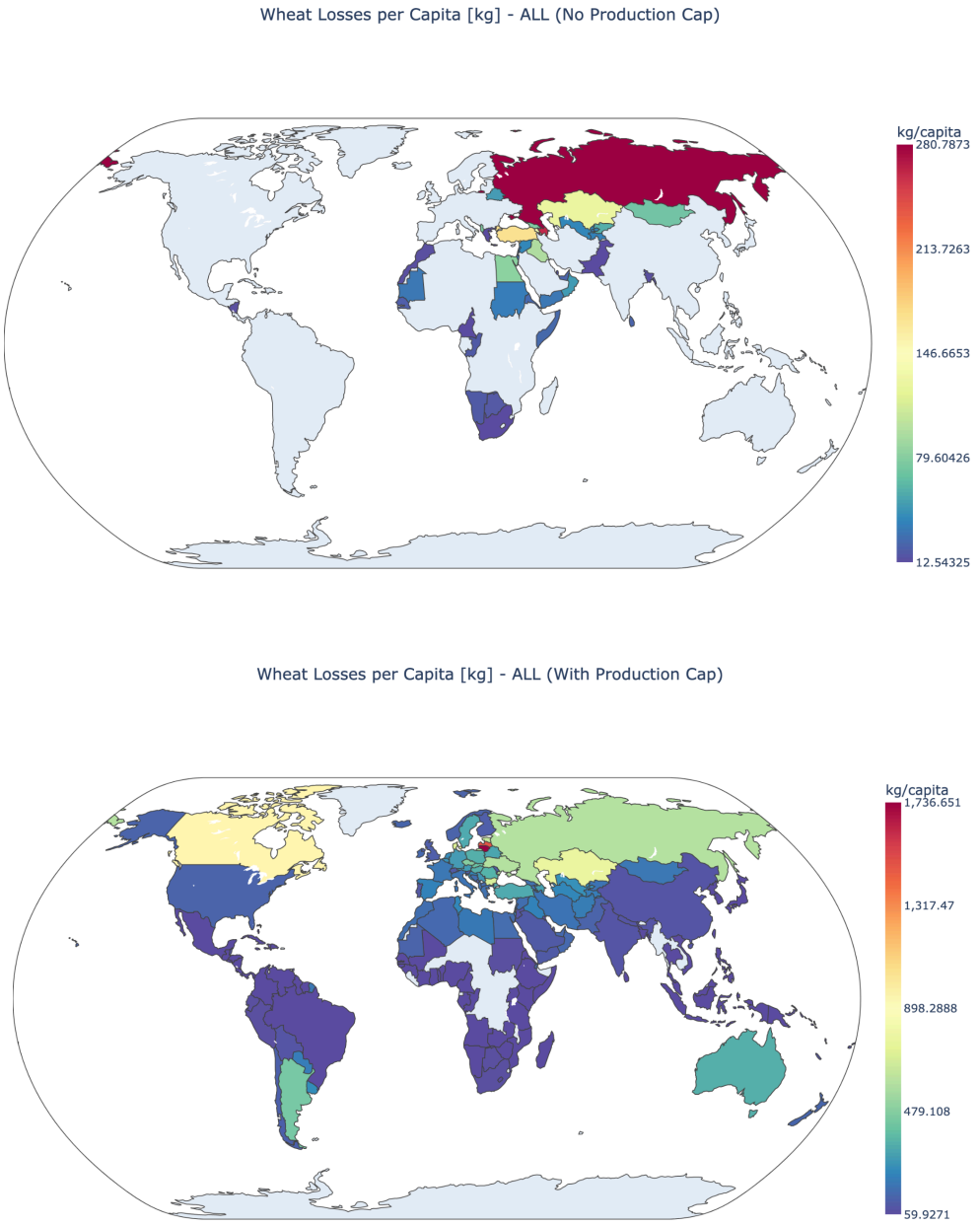

Figure 7: Global distribution of absolute losses per capita (kg/capita) for wheat and derived products, following the compound climate shock scenario, without a global production cap (top) and with a global production cap (bottom). Losses are calculated as the difference from amounts in the year before the disaster. Note the scale on the right hand side.

Both figures show that the losses significantly increased once a global production cap was introduced. *Figure 6* shows that while only China and Ethiopia suffered significant losses of more than 10 kg per capita for only three products, once a global production cap is introduced, the amount of countries and products affected are significantly larger. The impact of the production cap is further highlighted by its impact on the losses of wheat after the compound shock event. Without the global production cap, the most affected country is

Russia, with a loss of approximately 280 kg per capita. The number of affected countries is also comparatively low and the most affected regions are concentrated in Northern and Western Asia and Africa. Once the global production cap is introduced, virtually all countries, with the exception of landlocked subsaharan Africa, are affected by losses in wheat. Interestingly, the most affected country now is Lithuania, which was not affected before the cap was introduced, suffering a loss of 1736 kg per capita of wheat. Russia in this case only suffers losses of around 500 kg per capita, less than before the cap was introduced. These changes are due to the adaptation and rewiring process, that is forced to respect a predetermined planetary limit, and cannot compensate by indefinitely scaling up production. Such losses are highly significant, considering that in countries across the world, yearly wheat consumption per capita may rise to over 200 kg. For example, in 2021 Russia consumed 138 kg of wheat per person, whereas Lithuania 107 kg (see FAOSTAT food balances: FAO, 2025). The projected losses could therefore be devastating, if not properly compensated by substitutable products.

Our second hypothesis (H2) posited that introducing a realistic production cap would reduce the system's resilience by constraining adaptation options and thus lead to higher total losses, compared to the model run without a global production cap. This is indeed confirmed by our simulation results. When the global production cap is active, food availability decreases more significantly in both directly and indirectly affected countries. As visualized in the heatmaps and maps above, losses intensify when the system is no longer able to compensate shocks by scaling up production. Countries can no longer rely on internal production increases alone and must trade or substitute certain products, which become more competitive under constraints caused by climate disaster events. This highlights the importance of planetary boundaries and ecological limits and the need to account for biophysical boundaries in modeling adaptive capacity of countries. Substitution mechanisms help buffer the impacts to some extent, especially for highly substitutable products, but their effectiveness diminishes under a global production cap. In particular, products with few or no viable substitutes and that are necessary inputs for other products (e.g., grazing as animal feed, see Figure 6 bottom diagram) become major bottlenecks. The production cap, therefore, not only increases absolute losses but also redistributes vulnerabilities and items that are more versus items that are less substitutable

Winners and losers

A further line of inquiry explored the distributional effects of the adaptation process due to the climate shocks. It was already mentioned that the rewiring mechanism is able to absorb compound damages in a fashion that will not only avert superadditive losses but also lead to even smaller damages of the compound shock compared to a single shock in the model without production capacity. To further demonstrate this, the next figure represents profits, in other words, negative losses in the model without the production capacity. The damages push up production for other goods by an absurd magnitude.

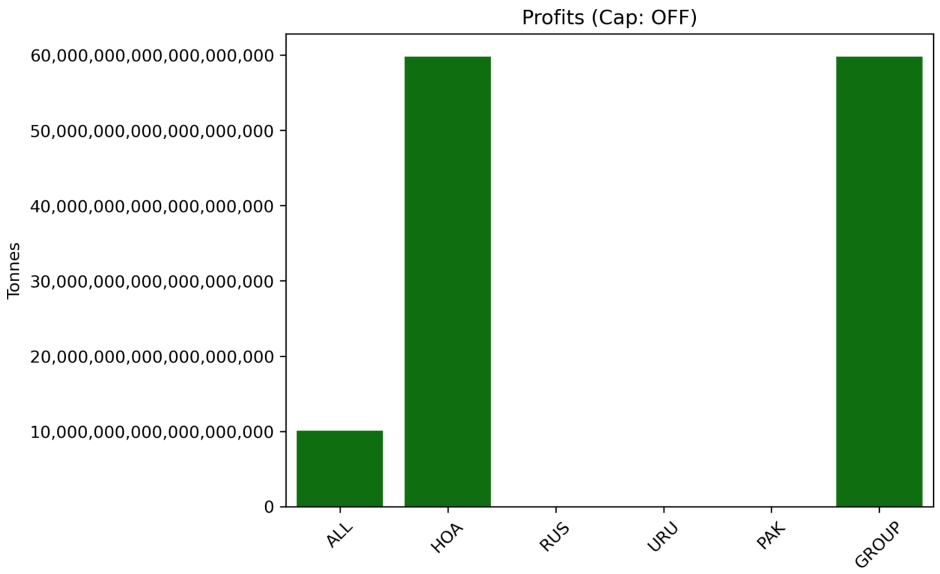

*Figure 8: Absolute profits in tonnes for the different scenarios without the global production cap. Close to **sixty quintillion.** This is equivalent to the amount of sand grains on beaches on Earth or stars in the observable universe.*

Compared to that the model with production capacity lowers that to more realistic magnitudes. Once a production cap is introduced, the absolute profits are much lower:

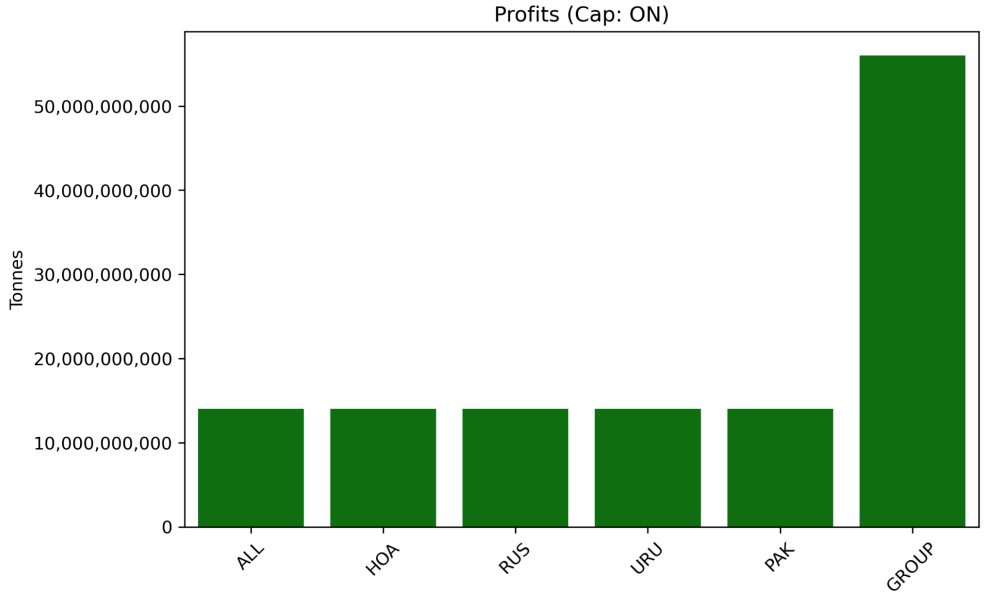

Figure 9: Absolute profits in tonnes in the model with the global production cap.

In the uncapped model (Figure 8), absolute food profits reached astronomically high levels. Such extreme values, driven by unconstrained global adaptation mechanisms, reflect the theoretical scope of the model, but fall outside any plausible planetary limits. Introducing a global production cap (Figure 9) dramatically reduces profits across all scenarios, which already demonstrates a first step towards more realistic results. This sharp difference underscores the importance of integrating biophysical limits into systems modeling to ensure

realistic outcomes. Furthermore, it seems that once the cap is introduced, the maximum profits are always the same value, demonstrating a maximum limit of additional food products that the network adaptation and rewiring is able to produce. Thus, the profits also do not scale in the compound shock event. Also, it is crucial to note that the profits are much lower than the losses displayed in Figure 5 above, showing that despite some country items combinations ending up with more volume after the climate shock events, the overall global availability of food is lower.

The next section discusses some limitations to our model and provides a critical evaluation.

Limitations and evaluation of model

We presented a complex, and yet simplified model for analyzing the impact of climate change disaster events on agricultural food production, and how such impacts propagate through the global food system. While it offers valuable insights, it's crucial to acknowledge several inherent limitations and areas for future refinement. We want to focus on four major limitations here.

First, a major limitation of our current model is its inability to fully capture the super-additive effects of compound climate shocks. In theory, when multiple climate-induced disaster events occur simultaneously or in close succession, their combined impact on global food systems may exceed the sum of their individual effects due to systemic interdependencies, cascading failures, and nonlinearities. However, our results show that the modeled losses from compound shocks (“ALL” scenario) are not greater than the sum of losses from individual shocks grouped together; they are smaller. This suggests that the model may either underestimate the complex interactions and amplification mechanisms that occur when multiple crises overlap, or that the adaptation mechanism within the model is sufficiently strong to compensate for the super-additive losses in global food production. Recognizing this limitation is crucial.

Second, an initial limitation stems from the coarse spatial and temporal resolution of the data employed to simulate the impacts of the disaster events. The use of annual national production data dilutes the short-term and local or regional effects of climate events, making their direct impact difficult to discern. For instance, a severe but short-lived flood might not be fully reflected in annual aggregates. Our reliance on annual data fails to capture these nuances. The data we relied on must also be viewed critically. We relied on data on agricultural production reported by member states to the Food and Agriculture Organization of the United Nations. The data may not necessarily align with independent assessments. While acknowledging these potential limitations, the FAO database remains one of the most comprehensive databases for global agricultural data (for more details see for example FAO, 2024).

Third, some of our assumptions must be critically evaluated as well. The exponential decay of a food shock event is currently just an estimate, and ideally, this parameter would be more firmly grounded in empirical observations of post-disaster recovery. Similarly, the production

cap is presently treated as an estimated and averaged macro-variable that isn't sector-specific. This simplification might not accurately reflect the varying production capacities and constraints across different agricultural products. Furthermore, the model does not include product prices, which is one if not the most important variable in our real-world food system (Baum et al., 2024, 15).

Fourth, the methodology for calculating relative and absolute losses from the data also may introduce a distortion. When comparing the disaster year's production only to the previous year, an outlier in that preceding year can significantly skew the perceived picture of the change in production. Future iterations could benefit from comparing losses against a longer-term trend or average output value to provide for a more robust baseline

Overall, our model, based on the work by Baum et al., extends the foundations for understanding the interplay between climate events and agricultural production, with a focus on compound events and cascading effects of shocks. While more work is needed to understand why the losses do not show super-additive properties in compound shock scenarios, addressing the abovementioned limitations will be crucial for developing a more precise model. Furthermore, it is important to include planetary boundaries in future models to add realism and make them relevant and applicable to global issues.

6. Conclusion

As highlighted in our introduction, we aim to better understand how climate change and climate change induced natural disasters may exacerbate vulnerabilities within the global food network and lead to significant losses. Our research question asked: *How do cascading effects from climate-driven compound shocks affect global food availability?* We developed two hypotheses to answer this research question and tested them by developing a dynamic multi-layer network model of global food production and trade by Baum et al. (2024). We hypothesized that compound climate hazards may lead to superadditive shocks, and that the introduction of a realistic global production cap limiting food production to more realistic levels, would exacerbate global losses in food.

As discussed above, we did not find the super-additivity in the losses. Especially when the global production capacity is not introduced, the network's adaptation and substitution mechanisms lead to results that point in the opposite direction. Compound shocks can have less of an impact than single shocks (compare, for example, "ALL" and "RUS" in Figure 4). We find that this is due to a lack of realism in the baseline model with regard to possible growth adjustments that are not properly controlled. Especially when the profits due to the adaptation and substitution mechanism are calculated, this becomes obvious. Extending the model to account for this poses a further avenue for future research.

Regarding the second hypothesis, we can say that the introduction of the production capacity damps the effects of unrealistic overcompensation. Losses have become more severe in some

regions, leading to an increase in global vulnerability to climate shock events. We also observe that losses are evenly distributed across scenarios, including the compound shock event. Again, no super-additivity of losses can be detected, but rather, the results suggest that the network is able to adapt to a stable level of losses in all the scenarios. Our second hypothesis is supported in that we can see a significant increase in losses compared to the scenario without the global production cap that becomes more pronounced in more vulnerable regions of the world. This suggests a first step in the right direction of making the model more realistic even though we can not support the claim of super-additive losses even with a global production capacity. We propose that this is again mainly due to the network's adaptation and substitution mechanism, which is able to absorb the losses no matter in which scenario and will adapt to a level of losses that is mainly driven by the dynamics of the production capacity.

To conclude, our model extension does not support the first hypothesis. The adaptation and rewiring mechanisms within the network are capable of absorbing the losses from a compound shock event, leading to counterintuitive results. We observe that once the adaptation mechanism is triggered, the system can enter a phase of seemingly endless growth. This system behavior is due to a lack of realism in the baseline model! To address this, we introduced a global food production cap. However, further refinement is needed to strengthen our model extension, specifically, by making the cap region and product specific. These improvements are essential if researchers and policy-makers aim to more accurately understand and predict the impacts of single and compound shock events on a fundamental resource: food. Without such specificity, we may misunderstand how climate disaster events supposedly ripple through the global food network, with severe direct and indirect consequences, and potentially underestimate the impact of climate change on food availability.

There are several further extensions that may address the limits of our model. First, one could change the baseline adaptation and rewiring mechanisms themselves. This was already done by Baum, et al. for the parameters, but the crucial point is that the substitutability mechanism leads to the establishment of new trade relations and the establishment of new sectors in the trading countries. This is not controlled in any way. A small boost in one trade relationship can cascade through the network like a domino effect. This drives up production and trade to astronomical heights. Moreover, we encourage researchers to further develop our model not only by addressing the above-mentioned limitations, especially the super-additive properties of food losses, but also by including additional dimensions. For example, to understand how climate effects may exacerbate existing inequalities by including the HDIs of countries (Baum et al., 2024). Another potential extension may be to introduce policy responses to food shocks, which may distort the global food trade network through additional subsidies or export bans or embargoes following a climate change induced disaster in a particular country. Another possible improvement is an external control mechanism that regulates overall output and not just production. For example, one could implement energy conservation in such a way that output can not exceed initial input into the network, accounting for efficiency improvements.

Bibliography

Baum, S. *et al.* (2024) 'Adaptive Shock Compensation in the Multi-layer Network of Global Food Production and Trade'. arXiv. Available at: https://doi.org/10.48550/arXiv.2411.03502.

Bruckner, M. *et al.* (2019a) 'FABIO—The Construction of the Food and Agriculture Biomass Input–Output Model', *Environmental Science & Technology*, 53(19), pp. 11302–11312. Available at: https://doi.org/10.1021/acs.est.9b03554.

Bruckner, M. *et al.* (2019b) 'FABIO—The Construction of the Food and Agriculture Biomass Input–Output Model', *Environmental Science & Technology*, 53(19), pp. 11302–11312. Available at: https://doi.org/10.1021/acs.est.9b03554.

Burkholz, R. and Schweitzer, F. (2019) 'International crop trade networks: the impact of shocks and cascades', *Environmental Research Letters*, 14(11), p. 114013. Available at: https://doi.org/10.1088/1748-9326/ab4864.

Clevy, J.F. and Evans, C. (2025) 'The Macroeconomic Impact of Droughts in Uruguay', *IMF Working Papers*, 2025(004), p. 1. Available at: https://doi.org/10.5089/9798400298059.001.

Cottrell, R.S. *et al.* (2019) 'Food production shocks across land and sea', *Nature Sustainability*, 2(2), pp. 130–137. Available at: https://doi.org/10.1038/s41893-018-0210-1.

Das, A.K. *et al.* (2025) 'The Impact of Flooding on Soil Microbial Communities and Their Functions: A Review', *Stresses*, 5(2), p. 30. Available at: https://doi.org/10.3390/stresses5020030.

Devereux, S. and Edwards, J. (2004) 'Climate Change and Food Security', *IDS Bulletin*, 35(3), pp. 22–30. Available at: https://doi.org/10.1111/j.1759-5436.2004.tb00130.x.

Distefano, T. *et al.* (2018) 'Shock transmission in the International Food Trade Network', *PLOS ONE*, 13(8), p. e0200639. Available at: https://doi.org/10.1371/journal.pone.0200639.

Estrada, E. (2024) 'What is a Complex System, After All?', *Foundations of Science*, 29(4), pp. 1143–1170. Available at: https://doi.org/10.1007/s10699-023-09917-w.

FAO (2021) *The impact of disasters and crises on agriculture and food security*. Rome, IT. Available at: https://doi.org/10.4060/cb3673en.

FAO (2023) *Pakistan: Floods response update, February 2023*. Food and Agriculture Organization of the United Nations. Available at: https://doi.org/10.4060/cc4663en.

FAO (2024) World Food and Agriculture – Statistical Yearbook 2024. FAO ; Available at: https://openknowledge.fao.org/handle/20.500.14283/cd2971en (Accessed: 27 June 2025).

FAO (2025) 'FAOSTAT Crops and livestock products'. Available at: https://www.fao.org/faostat/en/#data/QCL.

Gaupp, F. *et al.* (2020) 'Changing risks of simultaneous global breadbasket failure', *Nature Climate Change*, 10(1), pp. 54–57. Available at: https://doi.org/10.1038/s41558-019-0600-z.

Gephart, J.A. *et al.* (2016) 'Vulnerability to shocks in the global seafood trade network', *Environmental Research Letters*, 11(3), p. 035008. Available at: https://doi.org/10.1088/1748-9326/11/3/035008.

Hallegatte, S. (2015) 'The Indirect Cost of Natural Disasters and an Economic Definition of Macroeconomic Resilience'. Rochester, NY: Social Science Research Network. Available at: https://papers.ssrn.com/abstract=2626266 (Accessed: 20 June 2025).

Headey, D. (2011) 'Rethinking the global food crisis: The role of trade shocks', *Food Policy*, 36(2), pp. 136–146. Available at: https://doi.org/10.1016/j.foodpol.2010.10.003.

Heilemann, J. *et al.* (2024) 'Projecting impacts of extreme weather events on crop yields using LASSO regression', *Weather and Climate Extremes*, 46, p. 100738. Available at: https://doi.org/10.1016/j.wace.2024.100738.

Hultgren, A. *et al.* (2025) 'Impacts of climate change on global agriculture accounting for adaptation', *Nature*, 642(8068), pp. 644–652. Available at: https://doi.org/10.1038/s41586-025-09085-w.

Hunt, E. *et al.* (2021) 'Agricultural and food security impacts from the 2010 Russia flash drought', *Weather and Climate Extremes*, 34, p. 100383. Available at: https://doi.org/10.1016/j.wace.2021.100383.

Intergovernmental Panel On Climate Change (Ipcc) (2023) *Climate Change 2021 – The Physical Science Basis: Working Group I Contribution to the Sixth Assessment Report of the Intergovernmental Panel on Climate Change*. 1st edn. Cambridge University Press. Available at: https://doi.org/10.1017/9781009157896.

IPCC (2022) *Climate Change and Land: IPCC Special Report on Climate Change, Desertification, Land Degradation, Sustainable Land Management, Food Security, and Greenhouse Gas Fluxes in Terrestrial Ecosystems*. 1st edn. Cambridge University Press. Available at: https://doi.org/10.1017/9781009157988.

Laber, M. *et al.* (2023) 'Shock propagation from the Russia–Ukraine conflict on international multilayer food production network determines global food availability', *Nature Food*, 4(6), pp. 508–517. Available at: https://doi.org/10.1038/s43016-023-00771-4.

Lagi, M. *et al.* (2011) 'The Food Crises: A Quantitative Model of Food Prices Including Speculators and Ethanol Conversion'. Rochester, NY: Social Science Research Network. Available at: https://doi.org/10.2139/ssrn.1932247.

Nyström, M. *et al.* (2019) 'Anatomy and resilience of the global production ecosystem', *Nature*, 575(7781), pp. 98–108. Available at: https://doi.org/10.1038/s41586-019-1712-3.

Observatory of Economic Complexity (2025) *Rice in Pakistan Trade*, *The*. Available at: https://oec.world/en/profile/bilateral-product/rice/reporter/pak (Accessed: 23 June 2025).

Odongo, R.A. *et al.* (2025) 'Drought impacts and community adaptation: Perspectives on the 2020–2023 drought in East Africa', *International Journal of Disaster Risk Reduction*, 119, p. 105309. Available at: https://doi.org/10.1016/j.ijdrr.2025.105309.

OECD and FAO (2022) *OECD-FAO Agricultural Outlook 2022-2031*. OECD (OECD-FAO Agricultural Outlook). Available at: https://doi.org/10.1787/f1b0b29c-en.

Pieper, O. (2023) *Uruguay drought: Capital hit by water shortages – DW – 06/30/2023*, *dw.com*. Available at: https://www.dw.com/en/uruguay-drought-capital-montevideo-hit-by-water-shortages/a-66075991 (Accessed: 23 June 2025).

Pretty, J. *et al.* (2018) 'Global assessment of agricultural system redesign for sustainable intensification', *Nature Sustainability*, 1(8), pp. 441–446. Available at: https://doi.org/10.1038/s41893-018-0114-0.

Qamer, F.M. *et al.* (2023) 'A framework for multi-sensor satellite data to evaluate crop production losses: the case study of 2022 Pakistan floods', *Scientific Reports*, 13(1), p. 4240. Available at: https://doi.org/10.1038/s41598-023-30347-y.

Schewe, J., Otto, C. and Frieler, K. (2017) 'The role of storage dynamics in annual wheat prices', *Environmental Research Letters*, 12(5), p. 054005. Available at: https://doi.org/10.1088/1748-9326/aa678e.

Shi, W. *et al.* (2025) 'Projected increase in global compound agricultural drought and hot events under climate change', *Global and Planetary Change*, p. 104962. Available at: https://doi.org/10.1016/j.gloplacha.2025.104962.

Siegenfeld, A.F. and Bar-Yam, Y. (2020) 'An Introduction to Complex Systems Science and Its Applications', *Complexity*, 2020, pp. 1–16. Available at: https://doi.org/10.1155/2020/6105872.

Simpson, N.P. *et al.* (2023) 'Adaptation to compound climate risks: A systematic global stocktake', *iScience*, 26(2), p. 105926. Available at: https://doi.org/10.1016/j.isci.2023.105926.

Springmann, M. *et al.* (2018) ‘Options for keeping the food system within environmental limits’, *Nature*, 562(7728), pp. 519–525. Available at: https://doi.org/10.1038/s41586-018-0594-0.

Stehl, J. *et al.* (2025) ‘Gap between national food production and food-based dietary guidance highlights lack of national self-sufficiency’, *Nature Food*, pp. 1–6. Available at: https://doi.org/10.1038/s43016-025-01173-4.

USDA (2023) *Growth rate of global agricultural output has slowed | Economic Research Service*, *Unted States Department of Agriculture*. Available at: https://www.ers.usda.gov/data-products/charts-of-note/chart-detail?chartId=107931 (Accessed: 23 June 2025).

Van Loon, A.F. *et al.* (2024) ‘Review article: Drought as a continuum – memory effects in interlinked hydrological, ecological, and social systems’, *Natural Hazards and Earth System Sciences*, 24(9), pp. 3173–3205. Available at: https://doi.org/10.5194/nhess-24-3173-2024.

Wegren, S.K. (2011) ‘Food Security and Russia’s 2010 Drought’, *Eurasian Geography and Economics*, 52(1), pp. 140–156. Available at: https://doi.org/10.2747/1539-7216.52.1.140.

WMO (2023) *Another poor rainy season forecast for drought hit Horn of Africa*, *World Meteorological Organization*. Available at: https://wmo.int/media/news/another-poor-rainy-season-forecast-drought-hit-horn-of-africa (Accessed: 23 June 2025).

Annex 1: Code for adaptation mechanism

The code below written by Baum et al., 2024 demonstrates the adaptation mechanism:

```
# Check for events
   if t == 1 and compensation:

        change_rl = set(np.where(rl.toarray()[:, 0] > limit_rel_sim)[0])  # rl_shock
        change_al = set(np.where(al.toarray()[:, 0] > limit_abs_sim)[0])  # al_shock
        change = np.array(list(change_rl.intersection(change_al)))
        mask = np.isin(np.arange(Na * Ni), change)
```

Here we check whether there is an event so the conditions are met that the adaptation algorithm will be applied. The third condition, namely the coefficient of variation, is not yet included in the code from the official repository for the paper (adaptive_food_supply_network, GitHub) so we also did not apply it. When further pursuing the approach used here, it would need to implement it .

```
         alpha_shock[mask, :] = (alpha[mask, :].multiply(transition_alpha_multi[mask, :])
+
                                 transition_alpha_rewire[mask, :]).multiply(rl[mask])
        mask_2 = (alpha_shock.sum(axis=0).A1 > 0) & (
            (alpha_shock.sum(axis=0).A1 < alpha.sum(axis=0).A1 * 0.99) |
            (alpha_shock.sum(axis=0).A1 > alpha.sum(axis=0).A1 * 1.01)
        )
        alpha_shock[:, mask_2] = alpha_shock[:, mask_2].multiply(
            alpha.sum(axis=0).A1[mask_2] / alpha_shock.sum(axis=0).A1[mask_2])
```

Here the shock for the intermediate production process matrix α is computed and the dataframe manipulated so that it can be further applied later.

```
        beta_shock[mask, :] = (beta[mask, :].multiply(transition_beta_multi[mask, :]) +
                               transition_beta_rewire[mask, :]).multiply(rl[mask])
        mask_3 = (beta_shock.sum(axis=0).A1 > 0) & (
            (beta_shock.sum(axis=0).A1 < beta.sum(axis=0).A1 * 0.99) |
            (beta_shock.sum(axis=0).A1 > beta.sum(axis=0).A1 * 1.01)
        )
        beta_shock[:, mask_3] = beta_shock[:, mask_3].multiply(
            beta.sum(axis=0).A1[mask_3] / beta_shock.sum(axis=0).A1[mask_3])
```

The same here for the primary production process matrix β.

```
        nu_shock[:, mask] = (nu[:, mask].multiply(transition_nu_multi[:, mask]) +
                             transition_nu_rewire[:, mask]).multiply(rl[mask].T)
        mask_4 = (nu_shock.sum(axis=0).A1 > 0) & (
            (nu_shock.sum(axis=0).A1 < 0.99) | (nu_shock.sum(axis=0).A1 > 1.01)
        )
        nu_shock[:, mask_4] = nu_shock[:, mask_4] / nu_shock.sum(axis=0).A1[mask_4]
```

The same here for the input share matrix ν.

```
                                        eta_exp_shock[mask,     :]     =     (eta_exp[mask,
:].multiply(transition_eta_exp_multi[mask, :]) +
                                    transition_eta_exp_rewire[mask, :]).multiply(rl[mask])
```

η^{exp} corresponds to the share of the item that is exported.

```
                                      eta_prod_shock[mask,     :]     =     (eta_prod[mask,
```

```
:].multiply(transition_eta_prod_multi[mask, :]) +
                                                    transition_eta_prod_rewire[mask,
:]).multiply(rl[mask])
```

η^{prod} corresponds to the share of the item that is used for further production.

```
T_shock[mask, :] = (T[mask, :].multiply(transition_import_multi[mask, :]) +
                           transition_import_rewire[mask, :]).multiply(rl[mask])
       T_shock[:, mask] = (T[:, mask].multiply(transition_export_multi[:, mask]) +
                           transition_export_rewire[:, mask]).multiply(rl[mask].T)

       mask_5 = (T_shock.sum(axis=0).A1 > 0) & (
           (T_shock.sum(axis=0).A1 < 0.99) | (T_shock.sum(axis=0).A1 > 1.01)
       )
       T_shock[:, mask_5] = T_shock[:, mask_5] / T_shock.sum(axis=0).A1[mask_5]
```

T corresponds to the trade matrix

Code availability: The whole code repository can be found at: https://github.com/j-rigler/csm_project_/tree/Valentin

Annex 2: Product and commodity groups

Table A2: Product items and their respective commodity groups. Products within the same group can be substituted (Baum et al., 2024):

Commodity group	**Product Item**
Alcohol	Beer Beverages, Alcoholic Beverages, Fermented Wine
Ethano	Alcohol, Non-food
Oil cakes	Copra Cake Cottonseed Cake Groudnut Cake Oilseed Cakes, other Palmkernel, Cake Rape and Mustard Cake Sesameseed Cake Soyabean Cake Sunflowerseed Cake
Oil crops	Palm kernels
Sugar, sweeteners	Sugar (raw equivalent) Sugar non-centrifugal Sweeteners, other
Vegetable oils	Coconut Oil Cottonseed Oil Groundnut Oil Maize Germ Oil Oilcrops Oil, other Olive Oil Palm Oil Palmkernel Oil

	Rape and Mustard Oil Ricebran Oil Sesamesees Oil Soyabean Oil Sunflowerseed Oil
Fish	Fish, Seafood
Live animals	Asses Buffaloes Camelids, other Cattle Goats Horses Mules Pigs Poultry Birds Rabbits and hares Rodents, other Sheep
Animal fats	Fats, Animal, Raw
Eggs	Eggs
Hides, skins, wool	Hides and skins Silk Wool (clean equivalent
Honey	Honey
Meat	Bovine Meat Meat, other Mutton & Goat Meat Offals, edible Pigmeat Poultry Meat
Cereals	Barley and products Cereals, other Maize and products Millet and products Oats Rice and products Rye and products Sorghum and products Wheat and products
Coffee, tea, cocoa	Cocoa Beans and products Coffee and products Tea (including mate)
Fibre crops	Abaca Cotton lint Cottonseed Hard Fibres, other Jute Jute-Like Fibres Sisal Soft-Fibres, other
Fodder crops	Fodder crops

Grazing	Grazing
Oil crops	Coconuts (including Copra) Groundnuts Oil, palm fruit Oilcrops, other Olives (including preserved) Rape and Mustardseed Seed cotton Sesame seed Soyabeans Sunflower seed
Roots and tubers	Cassava and products Potatoes and products Roots, other Sweet potatoes Yams
Sugar crops	Sugar beet Sugar cane
Tabacco, rubber	Rubber Tobacco
Vegetables, fruit, nuts, pulses, spices	Apples and products Bananas Beans Citrus, other Cloves Dates Fruits, other Grapefruit and products Grapes and products (excluding Wine) Hops Lemons, Limes and products Nuts and products Onions Oranges, Mandarines Peas Pepper Pimento Pineapples and products Plantains Pulses, other and products Spices, other Tomatoes and products Vegetables, other

Annex 3: Code for substitution mechanism

The code below written by Baum et al., 2024 demonstrates the substitution mechanism:

```
if t == 2 and compensation:
```

```
        change_rl = set(np.where(rl.toarray()[:, 0] > limit_rel_sim)[0])
        change_al = set(np.where(al.toarray()[:, 0] > limit_abs_sim)[0])
        change = np.array(list(change_rl.intersection(change_al)))
        mask_subs = np.isin(np.arange(Na * Ni), change)
```

We check again whether the conditions are met.

```
        mask_subs_2 = substitutability_trade[mask_subs].nonzero()[1]

        T_shock[mask_subs_2, :] = T_shock[mask_subs_2, :].multiply(
            sprs.csr_matrix(substitutability_trade[mask_subs].data + 1).T)

        mask_subs_3 = (T_shock.sum(axis=0).A1 > 0) & (
            (T_shock.sum(axis=0).A1 < 0.99) | (T_shock.sum(axis=0).A1 > 1.01)
        )
                        T_shock[:,    mask_subs_3]    =    T_shock[:,    mask_subs_3]    /
T_shock.sum(axis=0).A1[mask_subs_3]
```

The substitutability mechanism is then applied if the conditions are met in $t = 2$.

Annex 4: Shocked products and magnitude for four climate induced disaster events

Table A4: Shock magnitude for highest affected products per country in each disaster event:

Country	Event	Product	Shock Magnitude (Φ)
Pakistan	Flood 2022	Rice and products	0.2146
Pakistan	Flood 2022	Cottonseed	0.4124
Pakistan	Flood 2022	Rape and Mustardseed	0.27
Pakistan	Flood 2022	Peas	0.29
Pakistan	Flood 2022	Dates	0.7274
Russia	Drought 2010	Wheat and products	0.3276
Russia	Drought 2010	Barley and products	0.533
Russia	Drought 2010	Cereals, Other	0.3985
Russia	Drought 2010	Maize and products	0.2216
Russia	Drought 2010	Oats	0.4039
Russia	Drought 2010	Peas	0.2344
Russia	Drought 2010	Potatoes and products	0.3208
Russia	Drought 2010	Rye and products	0.6225
Horn of Africa	Drought 2021–2023	Sugar cane (Kenya, 2023)	0.3686
Horn of Africa	Drought 2021–2023	Sorghum (Ethiopia, 2021)	0.2133
Horn of Africa	Drought 2021–2023	Tea (Kenya, 2021)	0.203
Horn of Africa	Drought 2021–2023	Tomatoes (Kenya, 2021)	0.3288
Horn of Africa	Drought 2021–2023	Milk (Ethiopia, 2021)	0.1762
Horn of Africa	Drought 2021–2023	Sugar cane (Ethiopia, 2021)	0.394
Horn of Africa	Drought 2021–2023	Sweet potatoes (Ethiopia, 2021)	0.4285

Horn of Africa	Drought 2021–2023	Pineapples (Kenya, 2023)	0.6146
Horn of Africa	Drought 2021–2023	Millet (Ethiopia, 2022)	0.2268
Horn of Africa	Drought 2021–2023	Sorghum (Kenya, 2021)	0.559
Horn of Africa	Drought 2021–2023	Eggs (Kenya, 2022)	0.9593
Horn of Africa	Drought 2021–2023	Wheat (Kenya, 2023)	0.1606
Horn of Africa	Drought 2021–2023	Groundnuts (Ethiopia, 2021)	0.3208
Horn of Africa	Drought 2021–2023	Millet (Kenya, 2021)	0.6132
Horn of Africa	Drought 2021–2023	Rice (Ethiopia, 2022)	0.2588
Horn of Africa	Drought 2021–2023	Sesame seed (Ethiopia, 2021)	0.4705
Horn of Africa	Drought 2021–2023	Honey (Ethiopia, 2021)	0.5976
Horn of Africa	Drought 2021–2023	Onions (Ethiopia, 2021)	0.3999
Horn of Africa	Drought 2021–2023	Lemons, Limes (Kenya, 2021)	0.3093
Horn of Africa	Drought 2021–2023	Onions (Kenya, 2021)	0.1675
Horn of Africa	Drought 2021–2023	Coconuts (Kenya, 2021)	0.2132
Horn of Africa	Drought 2021–2023	Beans (Djibouti, 2021)	0.25
Horn of Africa	Drought 2021–2023	Bovine Meat (Somalia, 2023)	0.0217
Uruguay	Drought 2021–2023	Soyabeans (2022)	0.7667
Uruguay	Drought 2021–2023	Maize (2021)	0.0442
Uruguay	Drought 2021–2023	Milk (2022)	0.0478
Uruguay	Drought 2021–2023	Sorghum (2022)	0.7157
Uruguay	Drought 2021–2023	Lemons, Limes (2022)	0.2746
Uruguay	Drought 2021–2023	Rice (2023)	0.018
Uruguay	Drought 2021–2023	Oranges, Mandarines (2023)	0.0728